

## Degradation Pathway of Dicyclanil in Water in the Presence of Titanium Dioxide. Comparison with Photolysis

GAËLLE GOUTAILLER,<sup>†</sup> CHANTAL GUILLARD,<sup>‡</sup> RENÉ FAURE,<sup>\*,‡</sup> AND  
 OLIVIER PAÏSSÉ<sup>§</sup>

Laboratoire des Sciences et Stratégies Analytiques (LSSA), Bât. Jules Raulin, Université Claude Bernard Lyon 1, 69622 Villeurbanne Cedex, France, Laboratoire de Photocatalyse, Catalyse et Environnement, Ifos, Ecole Centrale de Lyon, BP 163, 69131, Ecully Cedex, France, and Service Central d'Analyse (SCA), USR 059 CNRS-Echangeur de Solaize, BP 22, 69390 Vernaison, France

The solar photolytic behavior of the pesticide 4,6-diamino-2-cyclopropyl-pyrimidine-5-carbonitrile, currently known as dicyclanil, has been mimicked in a photoreactor operating with an artificial light flux. The rate and pathway of degradation were performed. An additional study, using TiO<sub>2</sub> photocatalysis, has been achieved in order to determine the efficiency of photocatalysis to degrade the molecule. The catalyst was titania Degussa P-25. The aim of this article was the identification of the intermediate products formed during the irradiation, to establish the degradation pathway of dicyclanil. The kinetics of the reactions were followed by liquid chromatography with a diode array detector (LC-DAD). Most of the organic compounds occurring during the photodegradation have been identified by means of liquid chromatography and mass spectrometry coupled techniques (HPLC-MS). Additional analyses were carried out to evaluate the mineralization rates into nitrate and ammonium ions.

**KEYWORDS:** dicyclanil; titanium dioxide; photolysis; photocatalysis; pesticide

### 1. INTRODUCTION

Dicyclanil (4,6-diamino-2-cyclopropyl-pyrimidine-5-carbonitrile) is a pyrimidine-derived insect growth regulator recently developed by Novartis Agro (**Figure 1**). It has been recommended for use on sheep and lambs (1–3). Applied at therapeutic doses of 30–100 mg kg<sup>-1</sup> bw with a ready-to-use 5% pour-on formulation, it is active in the prevention of myiasis or fly strike. It is mainly used in Australia, New Zealand, and South Africa (4–5). Dicyclanil has a long-lasting action which interferes with moulting and pupation in dipteran species. However, the precise mode of action of this compound on ectoparasites is not yet known (6).

The paucity of information concerning dicyclanil behavior in aqueous solutions prompted the initiation of this study. We wished to evaluate in the laboratory the behavior of the dicyclanil once submitted to ultraviolet light (a part of the solar light) and to propose a degradation pathway. Abiotic degradation by photolysis in aqueous solution is of interest to determining the impact of dicyclanil on the environment. Dicyclanil has no aquatic uses; however, it could potentially enter surface water by spray drift during application or runoff after application. A study relates that approximately 37–59% of the total dose

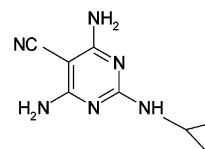


**Figure 1.** Structure of dicyclanil.

remained on the animals, the remainder being collected as runoff (6). Therefore, determination of the rate and route of photolytic degradation in water is crucial in defining the environmental impact of dicyclanil application.

We have investigated the degradation of dicyclanil from its aqueous solutions as a function of time, both by photolysis and photocatalysis. The latter was investigated in order to establish the ability of photocatalysis to degrade the dicyclanil. Indeed, photocatalytic oxidation is one of the emerging technologies for the elimination of organic compounds and their conversion into harmless chemicals (7–11). UV light absorption of the photocatalyst at a wavelength higher than that of the band gap, generates the creation of an electron–hole pair. The electron reduces the oxygen to form the radical anion O<sub>2</sub><sup>•-</sup>, while the hole h<sup>+</sup> reacts either directly with the pollutant or with water, leading to hydroxyl radicals OH<sup>•</sup>. These hydroxyl radicals are extremely reactive and readily attack organic molecules. They initiate a sequence of reactions resulting in partial or total destruction of these organic substrates and pollutants. The complete degradation leads to CO<sub>2</sub> and H<sub>2</sub>O and inorganic ions when the organic molecule contains other atoms.

\* Corresponding author. Tel: 00 (33) 4 72 43 11 53. Fax: 00 (33) 4 72 44 62 02. E-mail: faure@univ-lyon1.fr.

<sup>†</sup> Laboratoire des Sciences et Stratégies Analytiques.

<sup>‡</sup> Laboratoire de Photocatalyse.

<sup>§</sup> Service Central d'Analyse.

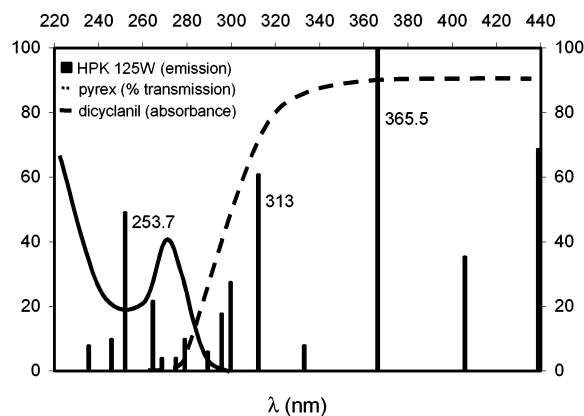


Figure 2. UV spectra of dicyclanil, Pyrex glass, and mercury lamp.

Many investigators have used different aqueous suspensions of semiconductor slurries. Among the semiconductors used, titanium dioxide ( $\text{TiO}_2$ ) is considered as a very efficient catalyst for the destruction of a wide variety of organic pollutants, including many pesticides in wastewater effluents as well as in polluted surface waters (12–13).

## 2. MATERIALS AND METHODS

**2.1. Chemicals.** Dicyclanil (purity 99.7%) was kindly provided by Ciba-Geigy (Novartis, Bâle, Switzerland) and used as received. The dicyclanil solutions were prepared by dissolving the pesticide in ultrapure water at an initial concentration of  $10 \text{ mg L}^{-1}$  ( $52.6 \mu\text{mol L}^{-1}$ ). Organic solvents were not used to aid the dissolution of the pesticide, to minimize any cosolvent effects on the photodegradation. Ultrapure water used for preparation of the stock solutions was filtered through a Milli-Q PLUS 185 water system (Millipore, Bedford, MA). The acetonitrile used for the liquid chromatography was of HPLC-grade (Rathburn, Walkerburn, Scotland).

All photocatalytic degradation assays were carried out using titanium dioxide "Degussa P25", which is predominantly anatase (80% anatase, 20% rutile). It is nonporous and offers a specific surface area of about  $50 \text{ m}^2 \text{ g}^{-1}$  and a density of  $3.85 \text{ g cm}^{-3}$ .

**2.2. Reactor and Light Source.** Irradiation was carried out with a high-pressure mercury lamp (Philips HPK 125 W), emitting in the wavelength range 250–600 nm, with a maximum emission at 360 nm. The measured flux of radiation was of  $54.3 \text{ mW cm}^{-2}$ . The lamp irradiated the reactor (85 mL) through its bottom. Between the lamp and the reactor, a circulating water Pyrex-glass tank cooler was positioned. The Pyrex-glass cutoff filter transmitting radiations longer than 290 nm was used in order to simulate a part of the solar radiation. The UV spectrum of the irradiating system and the absorption spectrum of dicyclanil are presented in Figure 2.

Constant agitation of the solution was ensured by a magnetic stirrer. The reactor remains open to the atmosphere allowing continuous contact between the water and air. It is noteworthy that the presence of oxygen and water is essential during the photomineralization process (14).

A 70 mL sample of dicyclanil solution (10 ppm) was used. Aliquots (800  $\mu\text{L}$ ) were taken at predetermined times of irradiation in order to follow the reaction. Irradiated samples were stored in the dark at  $-22 \text{ }^\circ\text{C}$  until analysis. A series of five or six runs was necessary to observe the whole degradation process. All experiments were carried out in triplicate.

**2.3. Experimental Procedure.** In the case of photocatalytic experiments, at the solution to be irradiated,  $700 \text{ mg L}^{-1}$  of  $\text{TiO}_2$  was added. This amount was determined to be optimum for the adsorption of all the incident efficient photons in our working conditions. The mixture was allowed to stay in the dark for 90 min under stirring to reach adsorption equilibrium, and then it was irradiated. Before analysis each sample was filtered in order to remove  $\text{TiO}_2$  particles. A  $0.45 \mu\text{m}$  filtration is used as titanium dioxide agglomerates in water, leading to particles of about one micrometer.

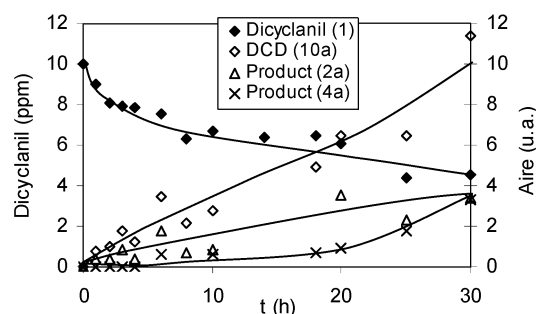


Figure 3. Photolysis of dicyclanil in aqueous solution (pH 6.2): irradiation with a Philips HPK 125W lamp.

**2.4. Analyses.** **2.4.1. Kinetic Studies.** All the experiments were conducted at room temperature in organic-free water (Milli-Q) and at natural pH (pH 6.2). The decrease of dicyclanil concentration during photolysis and photocatalysis, as well as the concomitant evolution of degradation products, was followed by direct injection of the aqueous samples into the liquid chromatographic system. The LC system used was a AS100 XR Thermoquest comprising a photodiode array detector. The analytical column used was a C18 (Spherisorb ODS2; length, 250 mm; internal diameter, 4.6 mm; particle size,  $5 \mu\text{m}$ ) provided from Interchrom. A water–acetonitrile (70/30; v/v) mixture, brought to pH 3 with phosphoric acid, was selected as the mobile phase. The eluent flow rate was fixed at  $1 \text{ mL min}^{-1}$ .

**2.4.2. Photoproducts Evaluation.** The intermediate products were identified by means of HPLC-MS (HP 1100 series LC MSD) with the ODS2 column. The mobile phase was a mixture of water, adjusted to pH 3 with trifluoroacetic acid, and acetonitrile (70/30; v/v). The UV detection was monitored from 210 to 300 nm, thanks to a photodiode array. Mass spectrometry detection was carried out in positive and negative electrospray modes.

**2.4.3. Mineralization Studies.** To follow the mineralization rate in the reactor, we examined the evolution of inorganic ions ( $\text{NO}_3^-$  and  $\text{NH}_4^+$ ) by LC using a Waters 501 pump and a Waters 431 conductivity detector. The  $\text{NO}_3^-$  ions were separated with a Sarasep AN1 ( $250 \times 4.6 \text{ mm}^2$  i.d.) column with a  $\text{NaHCO}_3$   $1.7 \cdot 10^{-3} \text{ mol L}^{-1}$ / $\text{Na}_2\text{CO}_3$   $1.8 \cdot 10^{-3} \text{ mol L}^{-1}$  mobile phase. The LC separation of  $\text{NH}_4^+$  ions was performed using a Chrompack Vydac IC 400 column ( $50 \times 4.6 \text{ mm}^2$  i.d.). The eluent was a  $\text{HNO}_3$   $2.5 \cdot 10^{-3} \text{ mol L}^{-1}$  aqueous solution, with a flow rate of  $1.5 \text{ mL min}^{-1}$ .

The  $\text{CN}^-$  and  $\text{CNO}^-$  ions were followed by ionic chromatography, with a Dionex apparatus. For the former the detection was amperometric, and for the latter it was a conductometric one.

**2.4.4. Identification of Carboxylic Acids.** The carboxylic acids were detected by LC using a Waters 600 pump and a Waters 486 UV detector fixed at 210 nm. The column was an Aminex ( $300 \times 7.8 \text{ mm}^2$  i.d.), and the mobile phase was a sulfuric acid aqueous solution ( $5 \cdot 10^{-3} \text{ mol L}^{-1}$ ) with a flow rate fixed at  $0.2 \text{ mL min}^{-1}$ .

## 3. RESULTS AND DISCUSSION

**3.1. Photolysis.** **3.1.1. Kinetics of Dicyclanil Disappearance.** The kinetic of the dicyclanil photolysis in aqueous solution is presented in Figure 3, with the concomitant appearance and evolution of three different photoproducts. The numbers in brackets refer to the degradation pathway a established in section 3.3.

When irradiated at  $\lambda > 290 \text{ nm}$ , a 10 ppm dicyclanil aqueous solution was degraded quite rapidly related to its UV spectra. After 30 h of irradiation, more than 48% of the initial dicyclanil decomposed. The initial slope of the curve indicates a degradation rate of  $0.81 \text{ mg L}^{-1} \text{ h}^{-1}$ .

The apparition and evolution of three photolytes have been followed by LC-UV during the degradation process. These intermediates have been identified by means of HPLC-MS as descyclopropylamino dicyclanil or 2,4,6-triamino-pyrimidine-

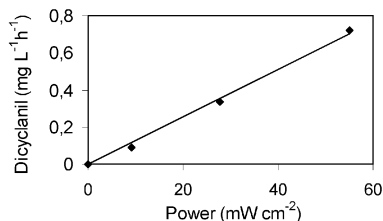


Figure 4. Influence of the irradiation power on the dicyclanil disappearance.

5-carbonitrile (noted as DCD, product 10a) ( $t_R = 9.6$  min), 3-amino-N-(4,6-diamino-pyrimidine-5-carbonitrile)-3-ol-propionaldehyde (product 2a) ( $t_R = 6.6$  min), and 3-amino-N-(4,6-diamino-pyrimidine-5-carbonitrile)-acetamide (product 4a) ( $t_R = 3.0$  min). All these photoproducts are not commercially available; hence, they could not have been quantified.

DCD results from the cleavage between the pyrimidic ring and the cyclopropylamino chain, whereas 2a and 4a are formed by the opening and oxidation of the cyclopropyl group. As product 4a appears after 6 h of irradiation, it can be considered as a secondary intermediate. The former derivative, descyclopropyl dicyclanil, has also been identified during metabolism of dicyclanil in rats (6).

In addition, we have established the influence of the irradiation power on the dicyclanil disappearance. The initial decrease of dicyclanil concentration is proportional to the radiation power (Figure 4). Considering that the mean solar power is  $4 \text{ mW cm}^{-2}$  (15), it can be estimated that the initial decrease of a 10 ppm dicyclanil solution in the environment would be about  $0.051 \text{ ppm h}^{-1}$ . However, this must be carefully extrapolated. First, the device used emits from 290 nm, whereas solar emission starts around 295 nm. In addition, dicyclanil can absorb more photons in the presence of solar light, as it emits a stronger continuous spectrum than our irradiating system. Second, natural water is not pure water but contains chromophores capable of affecting the reaction in many ways.

**3.1.1. Mineralization.** Mineralization of dicyclanil by photolysis results in the formation of both nitrate and ammonium ions. More ammonium ions are produced than nitrate ions; nevertheless, at 24 h of irradiation, the sum of both ions does not overcome 8% of the total amount corresponding to the entire mineralization of dicyclanil. This is in agreement with Figure 3, where the dicyclanil and its intermediates are still in solution after 24 h of irradiation. All these compounds possess six nitrogen atoms.

The mineralization into  $\text{CN}^-$  and  $\text{CNO}^-$  ions displays the formation of  $\text{CNO}^-$  ions at 6 h of irradiation ( $48 \mu\text{g L}^{-1}$ ). After 15 h of irradiation, they are no longer detected. The  $\text{CN}^-$  ions are not discerned during all the degradation conducted during 8 days.

**3.1.2. Formation of Carboxylic Acids.** The opening of the cyclopropyl ring gives simultaneously a series of carboxylic acids. Only formic and acetic acids have been identified by LC-UV.

**3.2. Photocatalysis.** **3.2.1. Kinetics of Dicyclanil Disappearance.** In the presence of titanium dioxide, the complete removal of dicyclanil from the solution was achieved within 45 min at irradiation wavelengths greater than 290 nm (Figure 5).

A first-order decomposition of the dicyclanil is observed. The calculated rate constant was  $0.092 \text{ min}^{-1}$ , and the calculated half-life was 7.5 min.

When  $\text{TiO}_2$  is used, the degradation rate is increased about 43 times compared to that of photolysis ( $35.3$  vs  $0.81 \text{ mg L}^{-1} \text{ h}^{-1}$ ).

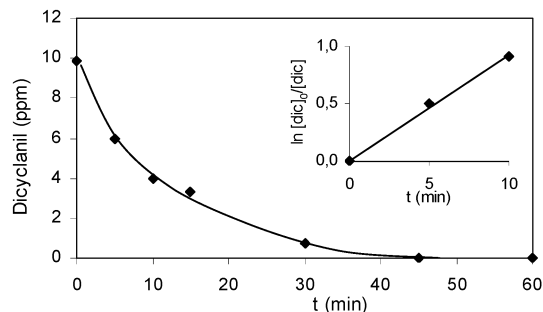


Figure 5. Photocatalysis of a 10 ppm aqueous solution of dicyclanil ( $700 \text{ mg L}^{-1} \text{ TiO}_2$ ).

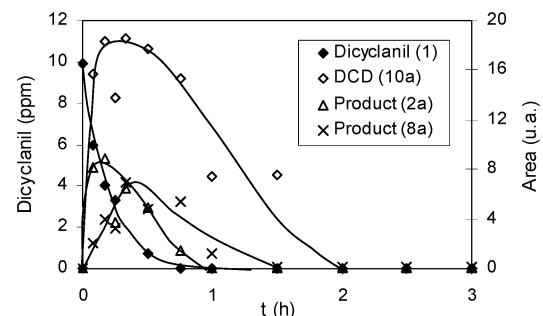


Figure 6. Intermediates evolution during photocatalysis of dicyclanil ( $700 \text{ mg L}^{-1} \text{ TiO}_2$ ).

**3.2.2. Nature and Evolution of the Intermediates.** The formation of DCD (product 10a) and of 3-amino-N-(4,6-diamino-pyrimidine-5-carbonitrile)-3-ol-propionaldehyde (product 2a), already observed during the photolytic process, is also detected in the presence of titanium dioxide (Figure 6). The degradation of both photoproducts is achieved in 2 h by photocatalysis, whereas by photolysis 30 h of irradiation were not sufficient to remove them.

The degradation of product 2a leads, by a series of oxidations and decarboxylations, to the 3-amino-N-(4,6-diamino-pyrimidine-5-carbonitrile)-formamide (product 8a). It is decomposed in 1 h 30.

**3.2.3. Mineralization.** During the first 3 h of the degradation, ammonium ions are produced in a much more extend than nitrate ions. This phenomenon has ever been observed in another study related to the photodegradation of pyrimidic rings substituted by  $\text{NH}_2$  groups (16). The initial formation of ammonium ions is probably due on one hand to the oxidation of the cyano group into an amido group (pathway c) which is known to generate ammonium ions and on the other hand to the oxidation of the  $\text{NH}_2$  groups (13, 17).

Unlike ammonium ions, nitrate ions are not primary products of the dicyclanil photocatalysis. They require 1 h of irradiation before being formed. Their production can be attributed either to the oxidation in solution of ammonium ions (18) or to the direct oxidation of  $\text{NH}_2$  ring substituents (13).

Chromatographic analyses coupled with conductometric and amperometric detection revealed the presence of  $\text{CN}^-$  and  $\text{CNO}^-$  ions, respectively. The quantities produced of both ions after 3 h of irradiation correspond to 20% of the quantity that would have been formed by the total mineralization of the cyano group of dicyclanil into these ions. It is noteworthy that  $\text{CN}^-$  ions are degraded and no longer detected after 6 h of irradiation.

**3.3. Proposed Degradation Pathway.** Schemes 1–3 propose pathways of the dicyclanil photodegradation. These schemes were established from the characterization of many photoproducts by HPLC-MS during the photocatalytic degradation. An

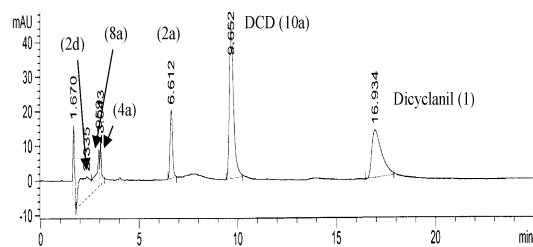
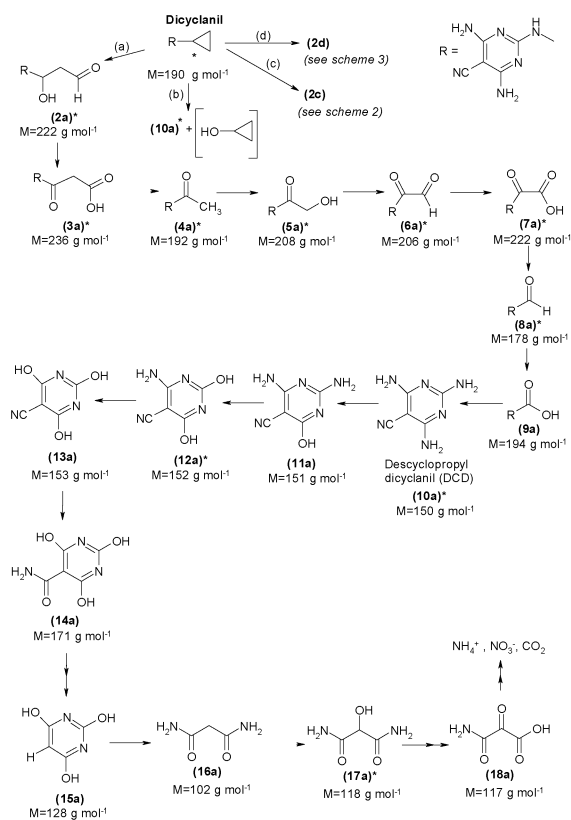


**Figure 7.** Typical HPLC-MS chromatogram obtained during the photocatalytic degradation of the dicyclanil. Numbers in parentheses refer to Scheme 1.

**Scheme 1.** Intermediates in the Photocatalytic Degradation of the Dicyclanil (Pathways a and b) (\*) Compounds Observed Both by Photocatalysis and Photolysis

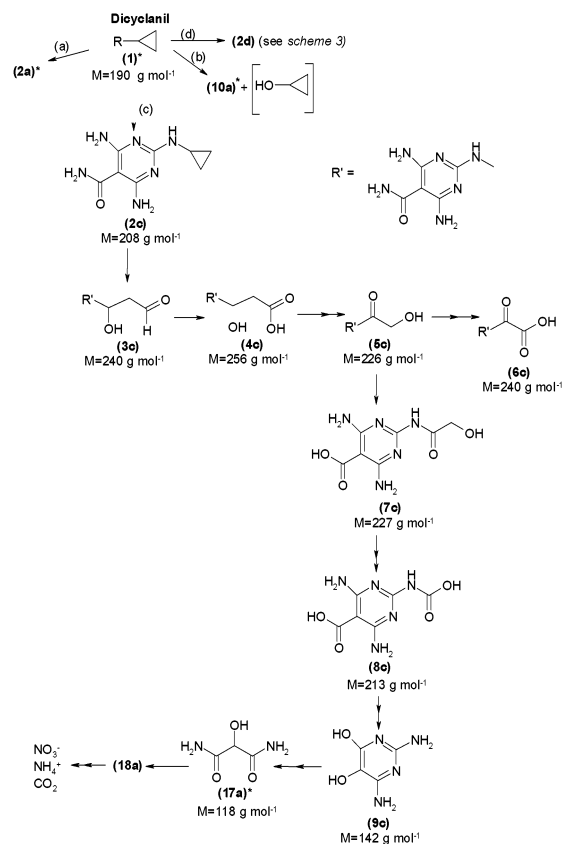


example of chromatogram is presented in **Figure 7**. Some of the photoproducts have also been detected during the photolysis process. These compounds are starred in the different schemes.

The LC-MS identified intermediates lead to consider four parallel pathways of degradation. The metabolites are characterized with electrospray ionization (positive mode) by their retention times ( $t_R$ ) and their molecular peaks ( $M + H$ ) and eventually their  $M + Na$  adduct peaks.

The first one (**Scheme 1**, pathway a) results from the oxidative opening of the cyclopropyl ring producing the aldehyde 2a ( $t_R = 6.601$  min;  $[M + H]$ ;  $[M + Na]$ ). This opening can be due, in photocatalysis, to an attack by  $OH^\bullet$  radicals, while in direct photolysis it can result either from a photoassisted hydrolysis or from the participation of singlet oxygen. The aldehyde 2a gives the  $\beta$ -ketoacid 3a ( $t_R = 4.020$  min;  $[M + H]$ ) which is decarboxylated into the methyl ketone 4a ( $t_R = 3.002$  min;  $[M + H]$ ;  $[M + Na]$ ). The decarboxylation process occurs by photocatalysis via reaction with the holes resulting from the excitation of the  $TiO_2$  semiconductor. By photolysis it arises from the formation of unstable acids which

**Scheme 2.** Intermediates in the Photocatalytic Degradation of the Dicyclanil (Pathway c) (\*) Compounds Observed Both by Photocatalysis and Photolysis

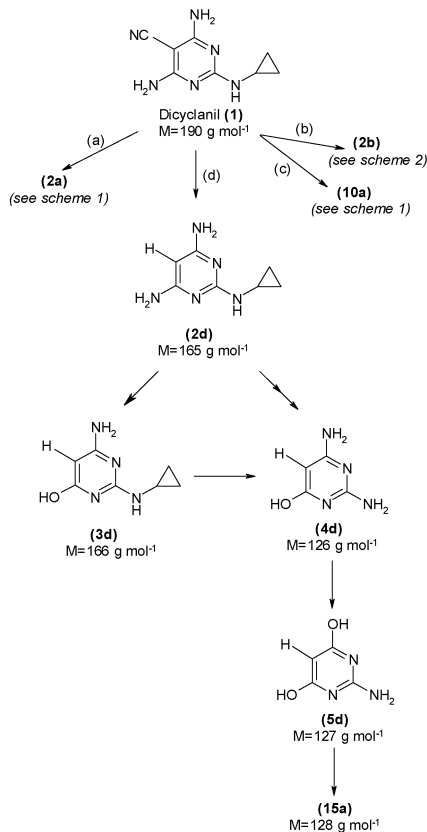


exist in the keto-enolic form and thus can absorb the ultraviolet radiation to be degraded (13). The product 4a is transformed into the  $\alpha$ -keto-alcohol 5a ( $t_R = 4.440$  min;  $[M + H]$ ) that is oxidized into the  $\alpha$ -keto-aldehyde 6a ( $t_R = 10.600$  min;  $[M + H]$ ) and then into the  $\alpha$ -keto-acid 7a ( $t_R = 1.800$  min;  $[M + H]$ ). The latter is decarboxylated into the aldehyde 8a ( $t_R = 2.960$  min;  $[M + H]$ ;  $[M + Na]$ ) that is converted into DCD through the acid 9a ( $t_R = 2.800$  min;  $[M + H]$ ) and consequently to an oxidation and a decarboxylation step. Next steps lead to compounds 11a ( $t_R = 2.400$  min;  $[M + H]$ ), 12a ( $t_R = 2.350$  min;  $[M + H]$ ), and 13a ( $t_R = 2.300$  min;  $[M + H]$ ) by successive hydroxylation of the pyrimidic ring. Then the cyano group of 13a is converted to the amide 14a ( $t_R = 2.100$  min;  $[M + H]$ ) that is oxidized and decarboxylated into 15a ( $t_R = 2.200$  min;  $[M + H]$ ;  $[M + Na]$ ). The oxidative opening of the pyrimidic ring composes the next step, giving the compound 16a ( $t_R = 9.400$  min;  $[M + H]$ ), which is oxidized into  $\alpha$ - $\alpha'$ -amido-alcohol (17a) ( $t_R = 5.200$  min;  $[M + H]$ ) and  $\alpha$ -keto- $\beta$ -amido-acid (18a) ( $t_R = 7.900$  min;  $[M + H]$ ). The opening of a pyrimidic ring has ever been observed by photocatalysis (19). The product 18a is then probably mineralized into carbon dioxide and ammonium ions.

In **Scheme 1**, pathway b leads directly to desiccyclopropyl dicyclanil 10a ( $t_R = 9.600$  min;  $[M + H]$ ) and consequently to an oxidative cleavage of the bond between the cyclopropyl ring and the exocyclic nitrogen.

Pathway c (**Scheme 2**) rises from the oxidation of the cyano group of the dicyclanil into amide 2c ( $t_R = 9.710$  min;  $[M + H]$ ). Then  $OH^\bullet$  radicals attack the cyclopropyl group to form the  $\beta$ -hydroxy-aldehyde 3c ( $t_R = 2.042$  min;  $[M + H]$ ). The latter is oxidized into  $\beta$ -hydroxy-acid 4c ( $t_R = 2.980$  min;  $[M + H]$ ), which is transformed into  $\alpha$ -keto-alcohol 5c ( $t_R = 3.040$



**Scheme 3.** Intermediates in the Photocatalytic Degradation of the Dicyclanil (Pathway d)

min; [M + H]; [M + Na]) and consequently to several oxidations and a decarboxylation processes. Then either the product 5c is oxidized into  $\alpha$ -keto-acid 6c ( $t_R = 2.040$  min; [M + H]), or its amide function is oxidized into an acid function 7c ( $t_R = 3.030$  min; [M + H]). This compound is oxidized and decarboxylated to give compound 8c ( $t_R = 2.026$  min; [M + H]; [M + Na]) and next compound 9c ( $t_R = 2.410$  min; [M + H]). After the opening of the cyclopropyl ring, the  $\alpha$ - $\alpha'$ -amido-alcohol (17a) is formed, which is submitted to the same route of degradation as pathway a.

In pathway d (**Scheme 3**) the first photoproduct (product 2d,  $t_R = 2.337$  min; [M + H]) results from the cleavage between the cyano group and the pyrimidic ring. This cleavage produces  $\text{CN}^-$  ions that are oxidized in solution into  $\text{CNO}^-$  ions. In samples irradiated for 3 h, both ions are detected at a concentration of 170 and  $132 \mu\text{g L}^{-1}$ , respectively. At longer irradiation time (6 h), only  $\text{CNO}^-$  is detected at a concentration of  $27 \mu\text{g L}^{-1}$ , which decreases below  $10 \mu\text{g L}^{-1}$  after 10 h. Then from product 2d, either one  $\text{NH}_2$  function is hydroxylated into 3d ( $t_R = 2.440$  min; [M + H]), or there is probably a cleavage between the exocyclic nitrogen and the cyclopropyl group, leading to a compound with three  $\text{NH}_2$  groups as substituents, but it has not been identified. However, its formation is suggested as the compound 4d ( $t_R = 9.000$  min; [M + H]) is identified, resulting from successive oxidations of compound 2d. It is noteworthy that the product 4d can also be produced from product 3d by the cleavage of the bond between the cyclopropyl ring and the nitrogen exocyclic. Then product 4d is hydroxylated into compound 5d ( $t_R = 10.013$  min; [M + H]; [M + Na]), which is in turn hydroxylated into compound 15a. The next steps are described in pathway a.

In conclusion, the dicyclanil is degraded both by photolysis and photocatalysis. The use of titanium dioxide allows to

accelerate more than 40 times the degradation and leads to the total destruction of the initial molecule of dicyclanil in less than 1 h. The use of HPLC-MS and LC-UV has permitted establishing a degradation scheme of dicyclanil under irradiation with and without the photocatalyst, including four different pathways. Some intermediates are observed both by photolysis and photocatalysis.

**LITERATURE CITED**

- (1) Nottingham, R. M.; Hosking, B. C.; Schmid, H. R.; Strehlau, G.; Junquera, P. Prevention of blowfly strike on coarse and fine woolled sheep with the insect growth regulator dicyclanil. *Aust. Vet. J.* **2001**, *79*, 51–57.
- (2) Lonsdale, B.; Schmid, H. R.; Junquera, P. Prevention of blowfly on lambs with the insect growth regulator dicyclanil. *Vet. Rec.* **2000**, *147*, 540–544.
- (3) Schmid, H. R.; Van Tulder, G.; Junquera, P. Field efficacy of the insect growth regulator dicyclanil for flystrike prevention on lambs. *Vet. Parasitol.* **1999**, *86*, 147–151.
- (4) Schmid, H. R.; Hyman, W. B.; DeBruin, C.; Van Zyl, A. P.; Junquera, P. Flystrike prevention on Merino lambs with the insect growth regulator dicyclanil. *S. Afr. Vet. Ver.* **2000**, *71*, 28–30.
- (5) Bowen, F. L.; Fisara, P.; Junquera, P.; Keevers, D. T.; Mahoney, R. H.; Schmid, H. R. Long-lasting prevention against blowfly strike using the insect growth regulator dicyclanil. *Aust. Vet. J.* **1999**, *77*, 454–460.
- (6) The European Agency for the Evaluation of Medicinal Products, Canary Wharf, London, UK. *Veterinary Medicines and Information Technology*; March 2000.
- (7) Pichat, P. In *Handbook of Heterogeneous Catalysis*; Ertl, G., Knozinger, H., Weitkamp, J., Eds; VCH: Weinheim, Germany, 1997; Vol. 4, pp 2111–2122.
- (8) Pichat, P.; Disdier, J.; Hoang-Van, C.; Mas, D.; Goutailler, G.; Gaysse, C. Purification/deodorization of indoor air and gaseous effluents by  $\text{TiO}_2$  photocatalysis. *Catal. Today* **2000**, *63*, 363–369.
- (9) Herrmann, J. M.; Guillard, C.; Arguello, M.; Aguera, A.; Tejedor, A.; Piedra, L.; Fernandez-Alba, A. Photocatalytic degradation of pesticide pirimiphos-methyl. Determination of the reaction pathway and identification of intermediate products by various analytical methods. *Catal. Today* **1999**, *54*, 353–367.
- (10) Malato, S.; Blanco, J.; Fernandez-Alba, A. R.; Aguera, A. Solar photocatalytic mineralization of commercial pesticides: acrinathrin. *Chemosphere* **2000**, *40*, 403–409.
- (11) Bianco Prevot, A.; Pramauro, E.; De la Guardia, M. Photocatalytic degradation of carbaryl in aqueous  $\text{TiO}_2$  suspensions containing surfactants. *Chemosphere* **1999**, *39*, 493–502.
- (12) Chiarenzelli, J. R.; Scudato, R. J.; Rafferty, D. E.; Wunderlich, M. L.; Roberts, R. N.; Pagano, J. J.; Yates, M. Photocatalytic degradation of simulated pesticide rinsates in water and soil matrices. *Chemosphere* **1995**, *30*, 173–185.
- (13) Goutailler, G.; Valette, J. C.; Guillard, C.; Paissé, O.; Faure, R. Photocatalysed degradation of cyromazine in aqueous titanium dioxide suspensions. Comparison with photolysis. *J. Photochem. Photobiol., A: Chem.* **2001**, *141*, 81–86.
- (14) Barbeni, M.; Pramauro, E.; Pelizzetti, E.; Borgarello, E.; Gratzel, M.; Serpone, N. Photodegradation of 4-chlorophenol catalyzed by titanium dioxide particles. *Nouv. J. Chim.* **1984**, *8*, 547–550.
- (15) Guillard, C.; Disdier, J.; Herrmann, J. M.; Lehaut, C.; Chopin, T.; Malato, S.; Blanco, J. Comparison of various titania samples of industrial origin in the solar photocatalytic detoxification of water containing 4-chlorophenol. *Catal. Today* **1999**, *54*, 217–228.
- (16) Horikoshi, S.; Hidaka, H. Photodegradation mechanism of heterocyclic two-nitrogen containing compounds in aqueous  $\text{TiO}_2$  dispersions by computer simulation. *J. Photochem. Photobiol., A: Chem.* **2001**, *141*, 201–207.

- (17) Horikoshi, S.; Serpone, N.; Yoshizawa, S.; Knowland, J.; Hidaka, H. Photocatalysed degradation of polymers in aqueous semiconductor suspensions. IV. Theoretical and experimental examination of constituent bases in nucleic acids at titania/water interfaces. *J. Photochem. Photobiol., A: Chem.* **1999**, *120*, 63–74.
- (18) Nohara, K.; Hidaka, H.; Pelizzetti, E.; Serpone, N. Processes of formation of  $\text{NH}_4^+$  and  $\text{NO}_3^-$  ions during the photocatalyzed oxidation of N-containing compounds at the titania/water interface. *J. Photochem. Photobiol., A: Chem.* **1997**, *102*, 265–272.
- (19) Aguera, A.; Almansa, E.; Tejedor, A.; Fernandez-Alba, A. R.; Malato, S.; Maldonado, M. I. Photocatalytic pilot scale degradation study of Pyrimethanil and of its main degradation products in waters by means of solid-phase extraction followed by gas and liquid chromatography with mass spectrometry detection. *Environ. Sci. Technol.* **2000**, *34*, 1563–1571.

---

**Received for review March 6, 2002. Revised manuscript received June 11, 2002. Accepted June 11, 2002.**

JF0202943